

# Lawrence Berkeley National Laboratory

## Lawrence Berkeley National Laboratory

**Title**

E-Cloud Driven Single-Bunch Instabilities in PS2

**Permalink**

<https://escholarship.org/uc/item/2cf3k7kt>

**Author**

Venturini, M.

**Publication Date**

2010-11-30

# E-CLOUD DRIVEN SINGLE-BUNCH INSTABILITIES IN PS2\*

M. Venturini<sup>†</sup>, M. Furman, G. Penn, R. Secondo, J-L. Vay, LBNL, CA 94720, USA  
R. De Maria, Y. Papaphilippou, and G. Rumolo, CERN, Geneva, Switzerland

## Abstract

One of the proposals under consideration for future upgrades of the LHC injector complex entails the replacement of the PS with the PS2, a longer circumference and higher energy synchrotron, with electron cloud effects representing a potentially serious limitation to the achievement of the upgrade goals. We report on ongoing numerical studies aiming at estimating the e-cloud density threshold for the occurrence of single bunch instabilities.

## INTRODUCTION

The requirement for PS2 is to accelerate bunch trains up to 50 GeV kinetic energy (twice the energy reach of PS) in either the 25 ns or 50 ns bunch spacing configurations, with  $4 \times 10^{11}$  and  $5.9 \times 10^{11}$  particles per bunch respectively.

In addition to space-charge effects [1] and classical instabilities [2], a potential limiting factor to the machine performance is the accumulation of electron cloud. E-cloud can affect the beam dynamics by triggering single or multi-bunch instabilities, or cause a growth of the beam emittance through incoherent effects. Extensive studies of electron cloud formation in the PS2 for various lattice elements, bunch trains structures and a range of assumptions concerning the secondary electron yield properties of the vacuum chamber are reported elsewhere [3]. Here we focus on a study investigating the potential impact of the electron cloud on the single-bunch dynamics. The investigation is being carried out essentially through macroparticle simulations using the Warp/POSINST code [4]. As an intermediate step toward a future analysis based on head-tail instability theory we also report on preliminary calculations of e-cloud induced wake functions carried out using the code POSINST [5].

Table 1: PS2 beam, lattice parameters (at extraction) used in the simulations

Kinetic energy (GeV)	50
Circumference (km)	1.34
Transverse tunes $\nu_{x,y}$	13.25, 8.2
Synchrotron tune $\nu_s$	$7.7 \times 10^{-4}$
Normlz'd emittance $\gamma\epsilon_{\perp}$ ( $\mu\text{m}$ )	6.5
Transverse rms sizes $\sigma_{x,y}$ (mm)	1.9, 1.8
Long. rms size $\sigma_z$ (m)	0.3
Transition gamma $\gamma_t$	35i
Slippage factor $\eta$	$-1.15 \times 10^{-3}$

\* Work supported by DOE under Contract No. DE-AC02-05CH11231 and the US LHC Accelerator Research Program (LARP).

<sup>†</sup> mventurini@lbl.gov

## SIMULATION MODEL AND RESULTS

The physics model used in our e-cloud macroparticle simulations as currently implemented in Warp/POSINST is similar to that implemented in [6]. In the model, beam/e-cloud interactions occur at a finite number of discrete interaction points (or ‘stations’) along the machine circumference, where electrons are effectively confined to a transverse plane orthogonal to the beam orbit. An initially cold and uniform electron distribution is assumed to exist before, and refreshed after, each bunch passage (but a more realistic distribution as determined, for example, by e-cloud build-up codes like POSINST [5], could also be accommodated). The electron dynamics during the bunch passage is determined by the self-fields and the fields generated by the beam particles, with an option to pin down the electron motion to vertical lines to mimic the dynamics in a dipole magnet. The dynamics of the beam particles is determined by their response to the electron fields at the stations in the ‘quasistatic’ approximation [4] and optionally to the beam’s own fields (space charge). However, in these simulations space charge effects of the beam on itself were turned off. The beam particles motion from station to station is modelled by linear transfer maps in the smooth approximation with chromatic effects accounted for by introduction of a phase-advance dependence on the particle momentum. The Poisson equation, yielding the fields generated by the electrons and the protons in the beam slices as the beam steps through each station, is solved on a rectangular grid with metallic boundary conditions enforced on the assumed aperture of the vacuum chamber. For the vacuum chamber sizes we assumed the tentative values  $2a=12$

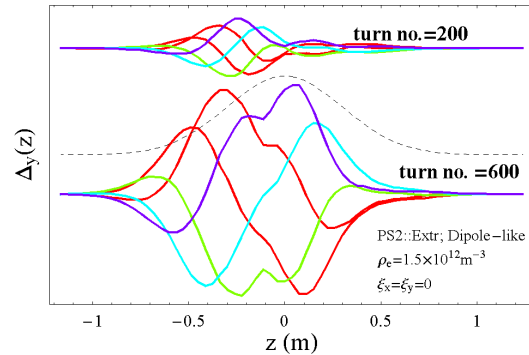


Figure 1: Beam vertical dipole moment monitored for 5 successive bunch passages starting from turn no. 200 and 600 above instability threshold. The dashed line represents the equilibrium bunch longitudinal profile. The beam head is at  $z > 0$ .

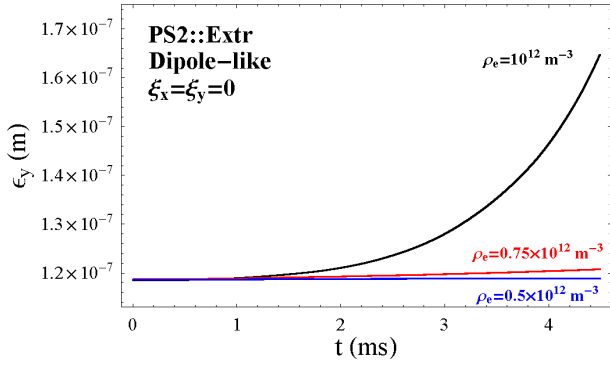


Figure 2: The electron motion is constrained to vertical lines (e-cloud in bending dipole magnets).

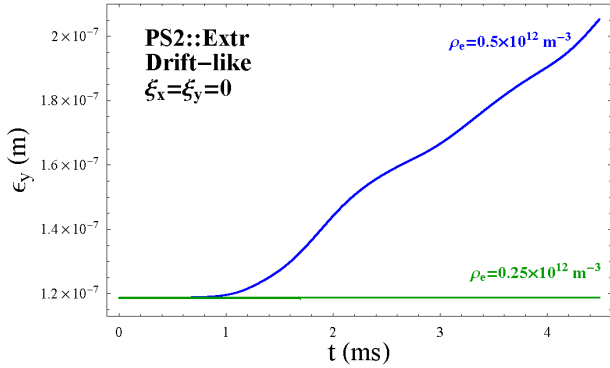


Figure 3: Electron motion is unconstrained (e-cloud in field-free regions).

and  $2b=7$  cm. We carried out two sets of simulations, with and without the option of pinning the electron motion to vertical lines. The two sets of simulations are intended to represent the beam dynamics in the approximation that the ring circumference is uniformly filled with the e-cloud pertaining to dipoles and drift elements of the physical machine. The more realistic scenario in which the electron density can vary along the machine, reflecting differences of e-cloud accumulation in dipoles and field-free regions, is left for future work.

Relevant machine parameters at extraction used in the present simulations are summarized in Table 1. The choice of the beam transverse sizes was made for consistency with earlier parameter assumptions for e-cloud build-up studies and does not necessarily reflect the current lattice design. These will be updated in future follow-up studies. Because of the difference in vertical and horizontal tunes, which in the smooth approximation set the betatron functions, the desired horizontal beam size was obtained by adjusting the value of the horizontal emittance (for the vertical emittance we used the nominal value indicated in Table 1). We assumed an initial gaussian beam distribution in the 6D phase space and kept the bunch population fixed to  $N_b = 5.9 \times 10^{11}$ .

The main goal of the study is to identify critical values of

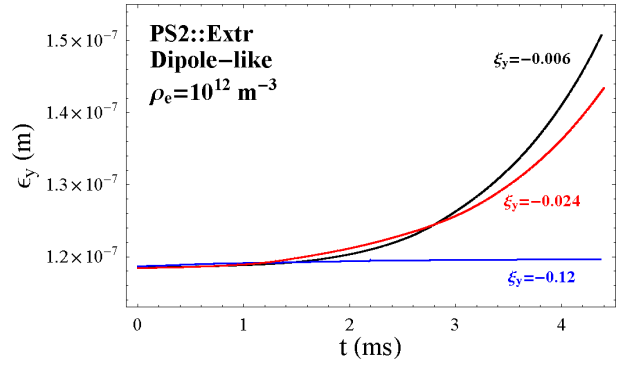


Figure 4: Negative chromaticities stabilize the motion.

the e-cloud density for the appearance of instabilities. We monitor these by inspection of the evolution of the beam emittance and centroids. Typical behavior of an unstable beam is illustrated in Fig. 1 where we show five turn-by-turn snapshots of the beam slices vertical centroid weighted by the beam longitudinal density after 200 and 600 turns, showing the increasing oscillation amplitude expected for head-tail like instabilities. The results of this simulation were obtained for the e-cloud density  $\rho_e = 10^{12} \text{ m}^{-3}$ . The instability was initiated by a uniform, small vertical beam offset. The apparent instability in the beam centroid is accompanied by emittance growth, see Fig. 2-4. In the simulations carried out so far, typically limited to about 1000 turns (or 4.6 ms), no emittance growth has been observed in the absence of the centroid motion instability. The threshold for the instability in the vertical plane was found to have a mild dependence on whether the option to confine the electron motion to vertical lines is enforced (dipole vs. drift-region like dynamics), varying from about  $\rho_e = 0.75 \times 10^{12} \text{ m}^{-3}$  in the first case (Fig. 2) to some value in the  $\rho_e = [0.25, 0.5] \times 10^{12} \text{ m}^{-3}$  range in the second case (drift-like motion), see Fig. 3. In the first case, as expected, the constraint on the electron motion suppresses any instability on the horizontal plane. In the second case a horizontal instability can develop but it appears at higher electron densities  $\rho_e \geq 10^{12} \text{ m}^{-3}$  (not shown). We tentatively ascribe this to the larger value of the horizontal betatron tune. As expected for head-tail like instabilities, a small chromaticity is shown to stabilize the centroid oscillations and reduce emittance growth (see Fig. 4). The (negative) sign of the stabilizing chromaticity is the same as the (negative) sign of the slippage factor. We verified that inverting the sign of the chromaticity does not cure and, in fact, may aggravate the instability.

The simulations were carried out using a fairly large number of macroparticles (500k) to represent the proton beam in order to stabilize the simulations outcomes from run to run. We found using about 20k macroelectrons to represent the electron cloud to be generally adequate, provided that the macroparticles are initially deposited on a regular grid. In most simulations we used 40 stations/turn

corresponding to 4 station/betatron wavelength in the vertical plane. Doubling the number of stations did not result in substantially different outcomes, at least in the few instances we considered. We subdivided the  $[-4\sigma_z, 4\sigma_z]$  longitudinal beam support into 64 slices.

## E-CLOUD INDUCED WAKE FUNCTIONS

A goal for future studies is to apply the linear theory for the Transverse Mode Coupling Instability (TMCI) in Perevedentsev's formulation [7]. This generalizes the conventional formalism to account for an arbitrary dependence of the wake function on the arguments  $z$  and  $z'$  (in the more conventional formulation it is assumed that the wake depends only on the difference  $z - z'$ ). The first step in the process entails evaluating the wake function, say in the vertical plane,

$$W_y(z, z') = -\frac{e\langle E_y(z) \rangle_{\perp}}{m_e c^2 r_e} \frac{L}{\langle y(z') \rangle_{\perp} N_b \rho(z') \Delta z'}. \quad (1)$$

This is determined from the component of the electron-generated electric field  $E_y(z)$  at position  $z$  trailing the position  $z' > z$  of the beam slice of length  $\Delta z$  with transverse offset  $\langle y(z') \rangle_{\perp}$  and local longitudinal density  $\rho(z')$  (normalized to unity). We show two examples of vertical wake functions calculated using POSINST, corresponding to the passage of a  $N_b = 5.9 \times 10^{11}$  proton bunch through a  $L=1$  m dipole with  $B_y = 1$  T. (Other relevant beam param-

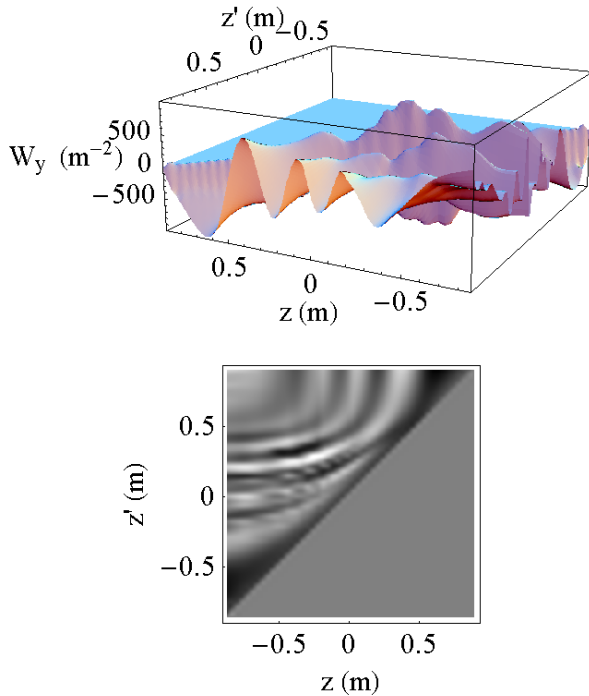


Figure 5: E-cloud induced wakefunction  $W_y(z, z')$  as calculated by POSINST evaluated for an initially uniform electron density with  $\rho_e = 10^{12} \text{ m}^{-3}$ .

eters are as in the Warp/POSINST simulations, but unlike the Warp/POSINST simulations the electrons here follow the correct gyromotion corresponding to  $B_y$ ). Fig. 5 shows the wake for an initially uniform electron distribution with density  $\rho_e = 10^{12} \text{ m}^{-3}$ ; Fig. 6 the wake for an electron distribution with initial gaussian transverse profile, peak density  $\rho_e = 10^{12} \text{ m}^{-3}$ , and same transverse rms sizes as the proton beam. The calculation was carried out for slice offsets equal to 1/4 of the beam transverse size. The calculation confirms that the wake profiles differ noticeably from, but are also reminiscent of, the profile expected for a broadband oscillator model, which is often used in approximate descriptions of e-cloud wakes.

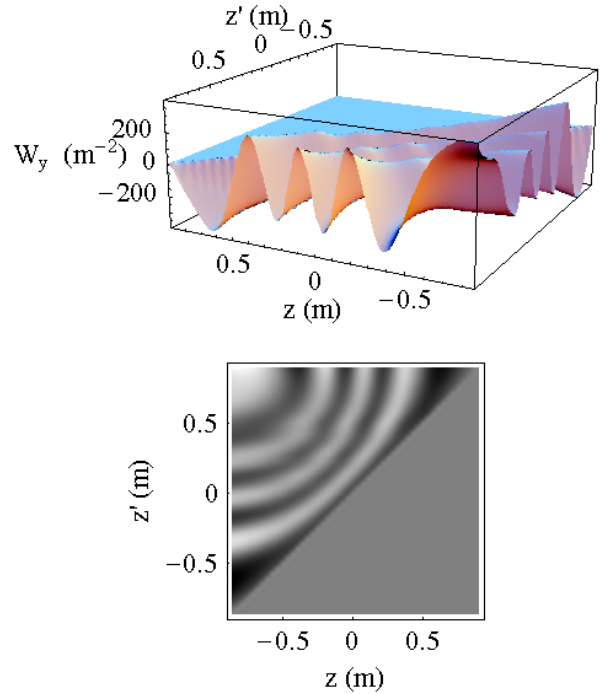


Figure 6: As in Fig. 5 but starting with a gaussian electron density.

## REFERENCES

- [1] J. Qiang *et al.*, Studies of Space Charge Effects in the Proposed CERN PS2, these proceedings.
- [2] K. Bane *et al.*, Impedance Considerations for the Design of the Vacuum System of the CERN PS2 Proton Synchrotron, these proceedings.
- [3] M. Furman *et al.*, Electron-cloud Build-up Simulations in the Proposed PS2: Status Report, these proceedings.
- [4] J-L Vay *et al.*, Update on E-Cloud Simulations using the Package Warp/Posinst, PAC09 Proceedings (2009).
- [5] M. Furman and M. Pivi, PRST-AB **5** 124404 (2002).
- [6] G. Rumolo and F. Zimmermann, PRST-AB **5** 121002 (2002).
- [7] E. Perevedentsev, E-CLOUD02 Workshop, Proceedings (2009).

This document was prepared as an account of work sponsored by the United States Government. While this document is believed to contain correct information, neither the United States Government nor any agency thereof, nor The Regents of the University of California, nor any of their employees, makes any warranty, express or implied, or assumes any legal responsibility for the accuracy, completeness, or usefulness of any information, apparatus, product, or process disclosed, or represents that its use would not infringe privately owned rights. Reference herein to any specific commercial product, process, or service by its trade name, trademark, manufacturer, or otherwise, does not necessarily constitute or imply its endorsement, recommendation, or favoring by the United States Government or any agency thereof, or The Regents of the University of California. The views and opinions of authors expressed herein do not necessarily state or reflect those of the United States Government or any agency thereof or The Regents of the University of California.